Biophysical Journal Volume 81 September 2001 1643–1656

Mechanics and Multiple-Particle Tracking Microheterogeneity of α-Actinin-Cross-Linked Actin Filament Networks

Yiider Tseng* and Denis Wirtz*†‡

*Department of Chemical Engineering, †Department of Materials Science and Engineering, and ‡Intercampus Program in Molecular Biophysics, The Johns Hopkins University, Baltimore, Maryland 21218 USA

ABSTRACT Cell morphology is controlled by the actin cytoskeleton organization and mechanical properties, which are regulated by the available contents in actin and actin regulatory proteins. Using rheometry and the recently developed multiple-particle tracking method, we compare the mechanical properties and microheterogeneity of actin filament networks containing the F-actin cross-linking protein α-actinin. The elasticity of F-actin/α-actinin networks increases with actin concentration more rapidly for a fixed molar ratio of actin to α-actinin than in the absence of α-actinin, for networks of fixed α-actinin concentration and of fixed actin concentration, but more slowly than theoretically predicted for a homogeneous cross-linked semiflexible polymer network. These rheological measurements are complemented by multiple-particle tracking of fluorescent microspheres imbedded in the networks. The distribution of the mean squared displacements of these microspheres becomes progressively more asymmetric and wider for increasing concentration in α-actinin and, to a lesser extent, for increasing actin concentration, which suggests that F-actin networks become progressively heterogeneous for increasing protein content. This may explain the slower-than-predicted rise in elasticity of F-actin/α-actinin networks. Together these in vitro results suggest that actin and α-actinin provides the cell with an unsuspected range of regulatory pathways to modulate its cytoskeleton's micromechanics and local organization in vivo.

INTRODUCTION

In nonmuscle cells, filamentous actin (F-actin)-cross-linking proteins organize cytoskeletal actin into extremely diverse, heterogeneous structures, including focal adhesions, dorsal arcs, and stress fibers in the cell body, and dendritic structures at the cell periphery (Borisy and Svitkina, 2000; Small et al., 1999). Immuno-fluorescence microscopy, electron microscopy, and micromechanical measurements have revealed that the distribution of F-actin cross-linking proteins in the cytoplasm (e.g., α-actinin) and associated mechanical properties are also heterogeneous (Svitkina and Borisy, 1999; Yamada et al., 2000; Merkel et al., 2000). Micromechanical measurements have recently demonstrated that the periphery of adherent cells is much stiffer and more solid-like than the perinuclear region (Yamada et al., 2000). However, the interplay between the local organization and the micromechanical strength of cytoskeletal actin and the local concentration in cross-linking proteins is unknown.

The expression patterns of actin and the ubiquitous F-actin cross-linking protein α-actinin, two proteins that co-localize to focal adhesions and stress fibers in adherent nonmuscle cells, are readily modulated by extracellular factors. These factors include insulin and extracellular matrix molecules, which modulate the level of expression of α-actinin (and other actin-binding proteins) and actin in nonmuscle cells (Gluck et al., 1992; Myers et al., 1999; Rodriguez Fernandez and Ben-Ze'ev, 1989; Kirkeeide et al., 1993). The regulation of α-actinin activity and actin polymerization by small molecules and cytoskeletal proteins (Pollard et al., 2000) can also provide the cell with supplemental pathways to control cytoskeleton mechanics and organization. Immunofluorescence microscopy shows that these changes in protein concentration typically correlate with a reorganization of the actin network. However, the mechanism by which changes in protein concentrations and associated changes in the F-actin cytoskeleton organization modulate cell micromechanics is not well understood.

Filamentous actin provides a large contribution to the stiffness of the cytoskeleton of an adherent cell. Nevertheless, a reconstituted network containing a physiological concentration of actin is much weaker than measured in vivo (Yamada et al., 2000; Palmer et al., 1999). This result implies that, to form a stiff architecture, F-actin requires auxiliary F-actin cross-linking proteins (Pollard et al., 1994). A recent theory (MacKintosh et al., 1995) which implicitly considers perfectly homogeneous networks predicts that an increase in F-actin concentration with a constant density of cross-linkers per polymer should create a very stiff network. However, as illustrated in Fig. 1, α-actinin can greatly affect the local homogeneity of an actin filament network, even in the absence of an external shear (Cortese and Frieden, 1988). Such microscopic heterogeneities, typically neglected by theoretical models, may in turn limit the rise in elasticity mediated by an increase in actin concentration and/or α-actinin concentration. Electron microscopy and rheometry reveal that α-actinin organizes actin filaments into stiff, orthogonal arrays at low concentra-

Received for publication 29 January 2001 and in final form 5 June 2001.

Address reprint requests to Denis Wirtz, Ph. D., Johns Hopkins University, Department of Chemical Engineering, Maryland Hall, Room 221, 3400 N. Charles Street, Baltimore, MD 21218. Tel.: 410-516-7006; Fax: 410-516-5510; E-mail: wirtz@jhu.edu.

0006-3495/01/09/1643/14 $2.00

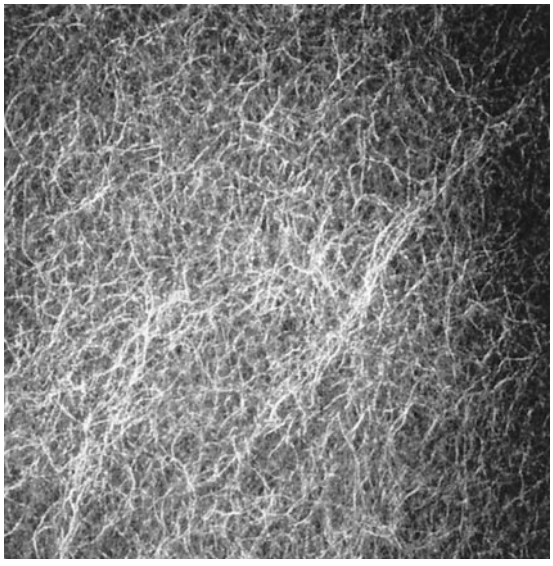

FIGURE 1 Confocal micrograph of an F-actin/α-actinin network. Twenty laser-scanned confocal sections 0.5 μm apart were combined into a maximum projection (see Methods). This figure shows a highly heterogeneous network containing a few large multifilament bundles imbedded in a dense meshwork of intertwined, thin bundles. Actin and α-actinin concentrations were 24 and 1.2 μM, respectively. The lower side of the figure represents 120 μm.

tions, and into relatively soft networks of filament bundles at high concentrations in vitro (Wachsstock et al., 1993; Grazi et al., 1993; Tempel et al., 1996). In part because of the absence of a quantitative method the effects of changing concentrations in F-actin and F-actin cross-linking proteins on the microheterogeneity of actin filament networks have not been studied.

This paper uses quantitative rheological methods and exploits the development of a novel approach, multiple-particle tracking (MPT; Apgar et al., 2000), to determine the relation between the degree of spatial heterogeneity and the mechanical properties of cross-linked actin filament networks. We consider three in vitro systems: F-actin/α-actinin networks of (I) constant actin concentration, (II) constant α-actinin concentration, and (III) constant molar ratio of actin-to-α-actinin. We find that these three systems exhibit different, and sometimes diametrically opposed, microstructural and mechanical behaviors for increasing protein content.

METHODS

Protein preparation

Actin was purified from chicken breast acetone powder (Spudich and Watt, 1971), followed by a gel-filtration step on Sephacryl S-300 HR as described (Xu et al., 1998d). The purified actin was stored as Ca^{2+}-actin and subjected to continuous dialysis at 4°C against buffer G (0.2 mM adenosine 5′-triphosphate, 0.5 mM dithiothreitol, 0.2 mM $CaCl_2$, 1 mM Na azide, and 2 mM Tris-HCl, pH 8.0). Filamentous actin (F-actin) was generated by mixing 9 volumes of actin in buffer G and 1 volume of 10× KMEI (500 mM KCl, 10 mM $MgCl_2$, 10 mM EGTA, 100 mM imidazole, pH 7.0). α-Actinin was purified from chicken gizzard as described (Xu et al., 1998d). Purified actin and α-actinin were used within 5 days after preparation.

Rheological methods

The mechanical properties of F-actin/α-actinin networks were measured using a cone-and-plate, strain-controlled rheometer (Rheometrics Instruments, Piscataway, NJ; Ma et al., 1999). Mixtures of G-actin and α-actinin were mixed with 10× KMEI, and gelation was monitored by recording the elastic modulus via application of a 4-s oscillatory deformation of 1 rad/s frequency and 1% amplitude every 30 s until steady state was reached. Because gelation (as measured by a rise in elasticity) did not follow an exponential behavior, the rate of gelation was conveniently defined as the inverse of the time required for reaching 90% of the steady state value of the elasticity. At steady state, the frequency-dependent elastic and loss moduli, $G'(\omega)$ and $G''(\omega)$, were measured by applying 1% amplitude oscillatory deformations of frequencies between 0.01 and 100 rad/s and measuring the in- and out-of-phase components of the resulting stress, respectively (Coulombe et al., 2000). Elastic and loss moduli are the ratios of the stress components to the amplitude of the applied deformation (= 1%). This paper reports the elastic modulus and the phase angle, $\delta(\omega) = \tan^{-1}[G''(\omega)/G'(\omega)]$, which characterizes the viscoelastic nature of the networks (see Results section). The mechanical measurements were conducted in the linear regime of small deformations, for which viscoelastic moduli and, supposedly, the polymer network ultrastructure are independent of the applied deformation. Large deformations can themselves reorganize the actin filament networks (Cortese and Frieden, 1988, 1990), a regime of deformations which was investigated in Xu et al. (2000).

MPT

To quantify the degree of spatial homogeneity of F-actin/α-actinin networks, the Brownian displacements of multiple microspheres dispersed in the network was measured via video light microscopy (Apgar et al., 2000; Ma et al., 2001). The principle of this new method extends the recently introduced method of particle tracking microrheology (Mason et al., 1997a, b; Gittes et al., 1997; Schnurr et al., 1997) to the measurement of the microheterogeneity of nonhomogeneous networks. A dilute suspension of 0.97-μm diameter, fluorescent, polystyrene (latex) microspheres (0.1 vol %) was mixed with each G-actin/α-actinin solution, which, after addition of 10× KMEI, was allowed to polymerize and gel overnight inside a PC20 CoverWell cell (Grace Bio-Labs, Bend, OR). Images of the microspheres were acquired as described (Leduc et al., 1999) using a SIT camera (VE-1000, Dage-MTI, Michigan City, IN) mounted on an inverted epifluorescence microscope equipped with a 100× magnification, 1.3 numerical aperture, oil-immersion lens (Nikon, Melville, NY). These images were analyzed using a custom subroutine incorporated into the software MetaMorph (Universal Imaging Corporation, West Chester, PA). The displacements of the centroids of individual microspheres were simultaneously tracked in the focal plane of the microscope for 50 s at a rate of 30 Hz, as many times as necessary to monitor a total of ~230 microspheres for each tested F-actin/α-actinin network. Our software can track hundreds of particles simultaneously, but the density of the microspheres was adjusted to limit the number of probe particles to 10–30 per field of view to reduce potential correlated interactions between neighboring particles. The spatial resolution, which was evaluated by tracking the apparent displacement of beads firmly tethered to the coverslip, was ~5 nm (Apgar et al., 2000). From the trajectories of the microsphere centroids, individual time-lag–averaged mean-square displacements (MSD), $\langle \Delta r^2(t) \rangle$, were computed (Palmer et al., 1998a, 1999; Xu et al., 1998c), from which time-lag–dependent MSD distributions were generated. These distributions were

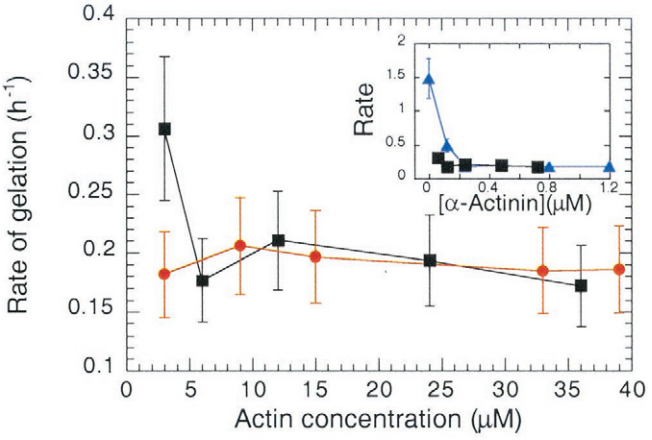

FIGURE 2 Concentration-dependent rate of gelation of F-actin/α-actinin solutions as a function of actin concentration. Symbols correspond to a fixed actin-to-α-actinin molar ratio of 50:1 (■) and to a fixed α-actinin concentration of 0.48 μM (●). (*Inset*) Gelation rate of F-actin/α-actinin solution as a function of α-actinin concentration. Symbols correspond to a fixed actin concentration of 24 μM (▲) and fixed actin-to-α-actinin molar ratio of 50:1(■). The rate is defined by the inverse of the time required to reach 90% of the steady state elasticity measured in a strain-controlled rheometer by subjecting the networks to 1% amplitude oscillatory shear deformations of 1 rad/s frequency (see Methods).

normalized by the time-lag–averaged, ensemble-averaged MSD and subsequently analyzed by computing median, standard deviation, and skewness, statistical parameters that describe the heterogeneity of the networks. The first proof of principle and more details about the implementation and use of MPT to quantitatively assess the microheterogeneity of biopolymer networks can be found elsewhere (Apgar et al., 2000).

Confocal fluorescence microscopy

Confocal fluorescence microscopy was used to qualitatively detect the heterogeneity of F-actin/α-actinin networks. Ten microliters of 6.6 μM rhodamine phalloidin (Molecular Probes, Eugene, OR) in methanol was deposited on the bottom of a PC20 CoverWell chamber (Grace Bio-Labs), and allowed to dry for 20 min. One volume of 10× KMEI, 1 M dithiothreitol, 0.18 mg/ml catalase, 1 mg/ml glucose oxidase, and 3 mg/ml glucose was added to nine volumes of the indicated final concentrations of actin and α-actinin in buffer G. The specimen was immediately placed in the microscopy chamber, allowed to gel overnight, and examined as described (Apgar et al., 2000) using a Nikon PCM2000 laser-scanning confocal system connected to a Nikon TE300 inverted microscope equipped with a 100× magnification, oil-immersion objective (numerical aperture 1.3). Using the software Simple PCI (Compix Inc. Imaging Systems, Cranberry Township, PA), 20 optical sections separated by 0.5 μm were collected and combined to generate a maximum projection of the F-actin/α-actinin network.

RESULTS

Gain in elasticity produced by an increase in actin concentration versus α-actinin concentration

We compared the gain in elasticity produced by the addition of actin, α-actinin, or both, to F-actin/α-actinin networks of

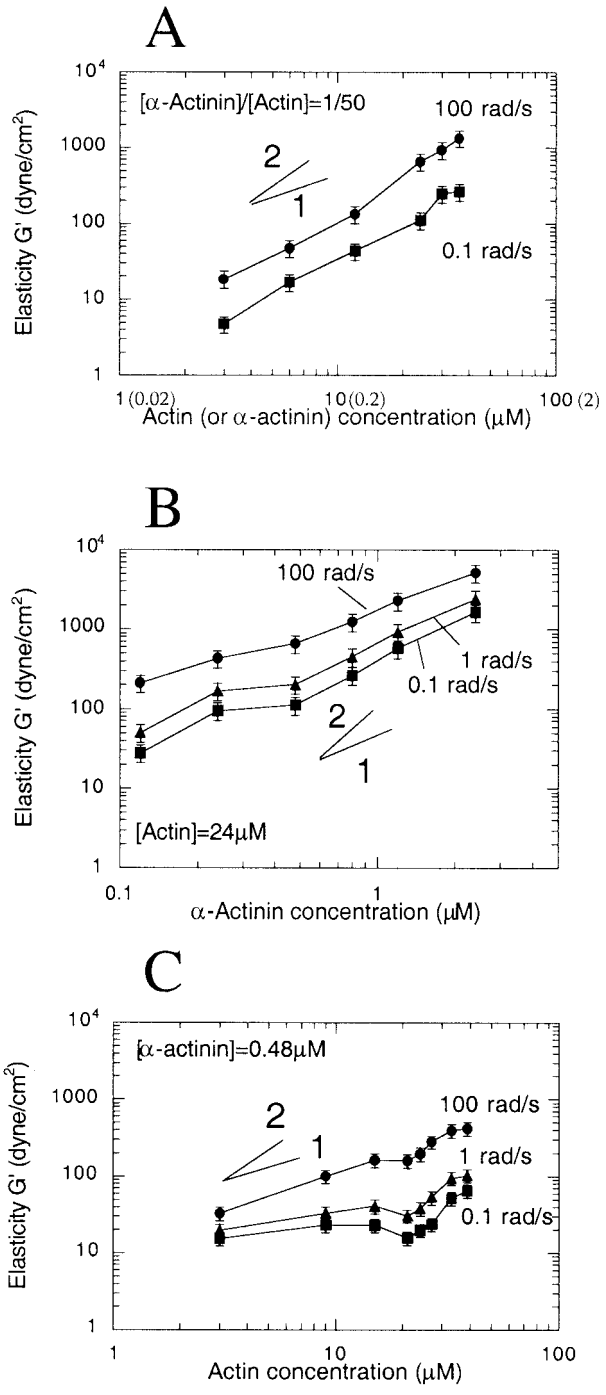

FIGURE 3 Concentration-dependent elasticity of F-actin/α-actinin networks. (*A*) Elastic modulus of F-actin/α-actinin networks of fixed molar ratio of actin-to-α-actinin as a function of actin (or α-actinin) concentration measured at different frequencies of deformation. The actin-to-α-actinin molar ratio was 50:1. (*B*) Elastic modulus of F-actin/α-actinin networks of fixed α-actinin concentration as a function of actin concentration. α-actinin concentration was 0.48 μM. (*C*) Elastic modulus of F-actin/α-actinin networks of fixed actin concentration as a function of α-actinin concentration. Actin concentration was 24 μM. Symbols in all figures correspond to deformation frequencies of 0.1(■), 1 (▲), and 100 rad/s (●). Elastic moduli were measured by a strain-controlled rheometer, which subjects the networks to 1% amplitude oscillatory shear deformations of controlled frequency and probes the in-phase component of the resulting stress (see Methods).

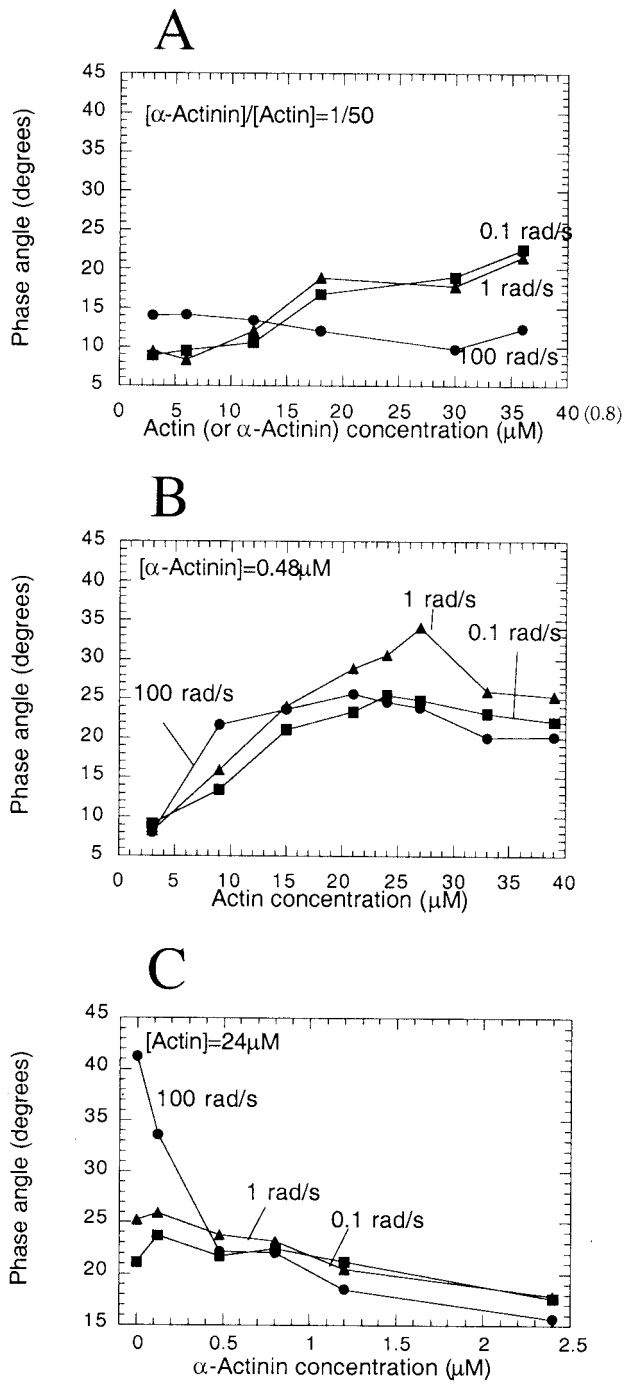

FIGURE 4 Concentration-dependent viscoelastic character (phase angle) of F-actin/α-actinin networks. (*A*) Phase angle of F-actin/α-actinin networks of fixed actin-to-α-actinin molar ratio as a function of actin (or α-actinin) concentration. (*B*) Phase angle of F-actin/α-actinin networks of fixed α-actinin concentration as a function of actin concentration. α-actinin concentration was 0.48 μM. (*C*) Phase angle of F-actin/α-actinin networks of fixed actin concentration as a function of α-actinin concentration measured. Symbols in *A–C* correspond to deformation frequencies of 0.1(■), 1 (▲), and 100 rad/s (●). Phase angles between the input strain and the output stress were measured by a cone-and-plate rheometer, which subjects the networks to 1% amplitude oscillatory deformations of various frequencies and probes the in- and out-of-phase components of the resulting stress (see Methods for rheological definitions).

1) constant actin concentration, 2) constant α-actinin concentration, or 3) constant molar ratio of actin-to-α-actinin. Interestingly, these three systems exhibited very similar concentration-dependent rates of network gelation (Fig. 2). The rate of gelation, measured by the inverse of the time required for reaching 90% of the steady state elasticity, was slightly lowered by the addition of actin to the networks (fixed α-actinin concentration, Fig. 2) and α-actinin (fixed actin concentration, *inset* in Fig. 2), but rapidly became concentration-independent for all three systems.

These systems showed, however, fundamentally different viscoelastic properties at steady state (Fig. 3–5). At a fixed molar ratio of actin-to-α-actinin of 50:1, for which actin filament networks formed orthogonal arrays (Wachsstock et al., 1993), the elastic modulus increased with actin concentration with an apparent power law, $G'(c_{actin}) \sim c_{actin}^{x}$, or, equivalently, scaled with α-actinin concentration as $G'(c_{\alpha\text{-actinin}}) \sim c_{\alpha\text{-actinin}}^{x}$ (Fig. 3 *A*). The exponent x, which characterizes the relative rate of increase of elasticity with protein concentration, was 1.71 ± 0.07 (mean ± standard deviation) for a deformation frequency of 1 rad/s, which is much higher than recently reported for F-actin networks in the absence of cross-linkers, for which $G'(c_{actin}) \sim c_{actin}^{1.27\pm0.22}$ (Palmer et al., 1999). The rate of increase of elasticity produced by the addition of α-actinin to F-actin/α-actinin networks of fixed actin content was slower: $G'(c_{\alpha\text{-actinin}}) \sim c_{\alpha\text{-actinin}}^{y}$ with $y = 1.24 \pm 0.05$ (Fig. 3 *B*). In striking contrast to these two systems, the elastic modulus of networks of fixed α-actinin concentration remained relatively constant and, past ~24 μM, increased slowly with actin concentration (Fig. 3 *C*). The level of elasticity generated in F-actin/α-actinin networks by increasing actin content and fixing α-actinin concentration was lower than those obtained by modulating α-actinin content (Fig. 3).

Viscoelastic character of F-actin/α-actinin networks

Modulation of the viscoelastic character of F-actin/α-actinin networks induced by changes in either actin or α-actinin concentrations was determined by measuring the phase angle, $\delta = \tan^{-1}(G''/G')$, which compares the storage (i.e., elastic) modulus to the loss (i.e., viscous) modulus. A phase angle of $\delta = 0°$, 90°, or between 0° and 90° describes a network which has the character of a Hookean solid (e.g., steel), a viscous liquid (e.g., oil), or a viscoelastic element, respectively (Ferry, 1980). For a fixed actin-to-α-actinin molar ratio, the phase angle of F-actin/α-actinin networks was almost constant at low actin concentrations, then increased from ~10 to 25° (ω = 1 rad/s) when actin concentration increased from 6 to 18 μM, and leveled off for actin concentrations >18 μM (Fig. 4 *A*). Because δ increased, the gain in viscosity in those F-actin/α-actinin networks was more rapid than the gain in elasticity. Nevertheless, because δ was systematically <45°, F-actin/α-actinin networks

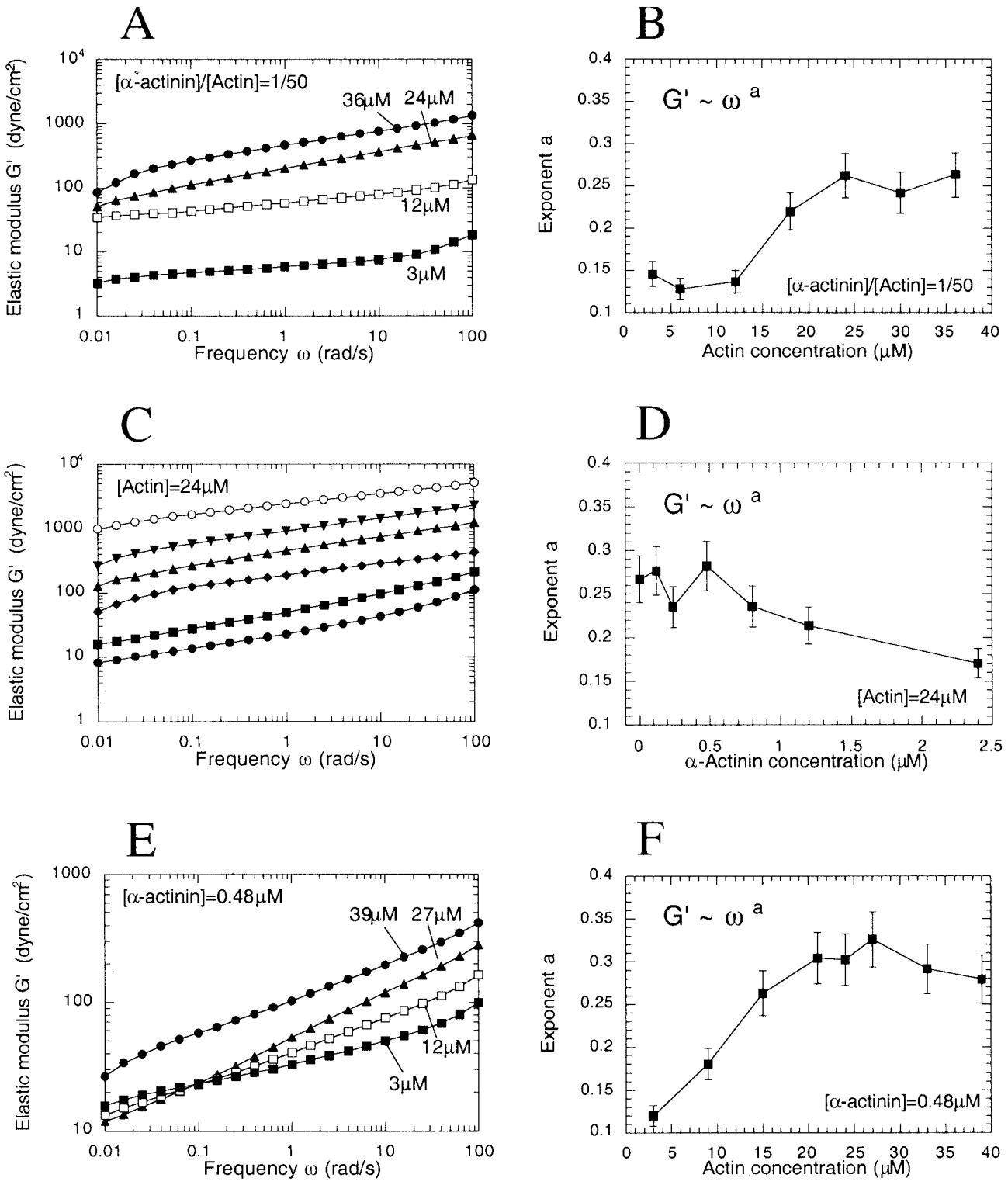

FIGURE 5 Frequency-dependent elasticity of F-actin/α-actinin networks. (*A*) F-Actin/α-actinin networks of fixed molar ratio of actin to α-actinin. α-actinin-to-actin molar ratio in all experiments was 1:50. Symbols correspond to 3 (■), 12 (□), 24 (▲), and 36 μM actin (●). (*B*) Dynamic exponent *a* of the elastic modulus of F-actin/α-actinin networks of fixed molar ratio of actin-to-α-actinin as a function of actin concentration. (*C*) F-Actin/α-actinin networks of fixed actin concentration. Actin concentration was 24 μM. Symbols correspond to 0.00 (●), 0.12 (■), 0.24 (◆), 0.80 (▲), 1.20 (▼), and 2.40 μM α-actinin (○). (*D*) Dynamic exponent of the elastic modulus of F-actin/α-actinin networks as a function of α-actinin concentration. (*E*) F-Actin/α-actinin networks of fixed α-actinin concentration. α-actinin concentration was 0.48 μM. Symbols correspond to 3 (■), 12 (□), 27 (▲), and 39 μM actin (●). (*F*) Dynamic exponent of the elastic modulus of F-actin/α-actinin networks as a function of actin concentration. Dynamical exponents *a* in *B*, *D*, and *F* were extracted from power-law fits of the frequency-dependent elastic modulus, $G'(\omega) \sim \omega^a$, for frequencies between 1 and 100 rad/s.

maintained a solid-like character even for actin concentrations as low as 3 μM (Fig. 4 *A*), for which filaments are expected to form few entanglements (Morse, 1998b). Interestingly, at high frequencies, the phase angle of F-actin/α-actinin networks monotonically decreased for increasing concentrations of actin and α-actinin (Fig. 4 *A*), i.e., when subject to high-rate deformations, the network became more solid-like for increasing concentrations both in F-actin and α-actinin. For networks of fixed α-actinin content, the phase angle of F-actin/α-actinin networks exhibited a distinct maximum at all tested frequencies, i.e., the network was progressively more liquid-like and then more solid-like (Fig. 4 *B*). Unlike these two other tested systems, an increasing concentration of α-actinin rendered F-actin/α-actinin solutions of fixed actin content systematically more solid-like at all tested frequencies, even for high α-actinin concentrations at which filament bundling became extensive (Wachsstock et al., 1993, 1994; Fig. 4 *C*). Therefore, the three tested α-actinin cross-linked actin filament networks displayed diametrically different viscoelastic behavior.

Actin filament dynamics in cross-linked networks

The regulation of the dynamics of actin filaments in solution (i.e., their propensity to diffuse and fluctuate, and, therefore, to relax the stress) was measured by subjecting networks to frequency-dependent deformations. This type of measurement mimics the response of the cytoskeleton to deformations of different rates (Sato et al., 1987; Xu et al., 2000; Maksym et al., 2000; Janmey et al., 1990). We observed that the three F-actin/α-actinin systems (fixed concentrations in actin or in α-actinin, and fixed protein molar ratio) behaved differently for increasing protein content. To compare the dynamic behavior of the filaments in various solutions, the frequency-dependent elastic modulus was fitted with power laws of the type $G'(\omega) \sim \omega^a$ for frequencies ω between 1 and 100 rad/s. The apparent exponent a characterizes the rate of change of elasticity. Note, however, that this exponent characterizes an intermediate frequency regime between the plateau regime at low frequencies and the high-frequency regime, which can be probed by laser tracking (Gittes et al., 1997; Schnurr et al., 1997; Yamada et al., 2000) and diffusing wave spectroscopy (Palmer et al., 1999; Xu et al., 1998a; Rufener et al., 1999). In the absence of α-actinin, an F-actin network exhibited a quasiplateau modulus at low frequencies and a large rate of increase in elasticity at high frequencies ($a = 0.26 \pm 0.03$). When actin and α-actinin concentrations were simultaneously increased, the rate of increase of elasticity (Fig. 5 *A*) as described by the exponent a, was initially constant ($\sim$0.15), then rapidly increased to $\sim$0.25 for actin concentrations between 15 and 25 μM, and became constant again for actin concentration higher than 25 μM (Fig. 5 *B*). This implies the somewhat surprising result that when the concentrations in filaments and cross-linkers are increased in concert, the relaxation of actin filaments in solution is accelerated, a behavior similarly observed in the actin cortex of living cells, which contains mixed structure of filaments and bundles (Yamada et al., 2000).

For a fixed actin concentration, the relaxation of the stress was progressively hindered for increasing concentration of α-actinin molecules per filament as a steadily decreased (Fig. 5, *C* and *D*). For F-actin networks of fixed α-actinin concentration, the profile of the elastic modulus became progressively more dependent on frequency (Fig. 5 *E*), i.e., the stress relaxed more rapidly for increasing concentration of actin (Fig. 5 *F*). This trend was however reversed at actin concentrations higher than $\sim$25 μM, for which a decreased. Therefore, the propensity of actin filaments to diffuse and fluctuate was accelerated and then decelerated for increasing concentration of polymers and a fixed concentration of α-actinin.

MSD distributions of polystyrene beads suspended in actin/α-actinin networks

We tested the hypothesis that polymer and cross-linker concentrations could control the heterogeneity of actin filament networks. Traditional approaches to measure microheterogeneity of a network, including electron and fluorescence microscopy (Fig. 1), are either qualitative or biased. After the recently developed method of MPT (Apgar et al., 2000), whose principle is illustrated in Fig. 6, the degree of heterogeneity of F-actin/α-actinin networks was quantified by measuring the range of Brownian displacements of dispersed microspheres. For each specimen, the trajectories of $\sim$230 randomly chosen, fluorescent, polystyrene microspheres suspended in the networks were recorded via video light microscopy (Fig. 6 *A*, *inset*) and analyzed by generating individual MSDs (Fig. 6 *A*). Median, standard deviation, and skewness of the MSD distributions (Fig. 6, *B* and *C*), normalized by the time-lag–dependent mean of the distribution, were extracted to evaluate the heterogeneity of the network as a function of actin or α-actinin concentration (Fig. 7–9 ; Apgar et al., 2000). We investigated whether the concentrations in polymers and cross-linkers could control the width and asymmetry of the MSD distribution, which measure the networks heterogeneity.

For a fixed molar ratio of actin-to-α-actinin, the amplitude of the Brownian motion of microspheres seemed typically to expand rapidly at short time scales and became restricted at long time scales (Fig. 6 *A*, *insets*). Accordingly, the MSD of the probe microspheres reached a quasiplateau at long time scales, i.e., past a characteristic time scale, the MSD increased slowly (Fig. 6 *A*), a behavior exacerbated at high actin concentrations (Fig. 7 *B*). This subdiffusive behavior ($\langle \Delta r^2(t) \rangle \sim t^\alpha$ where $\alpha < 1$) is consistent with a viscoelastic behavior (Palmer et al., 1999; Amblard et al., 1996). At a sufficiently low actin (and α-actinin) concen-

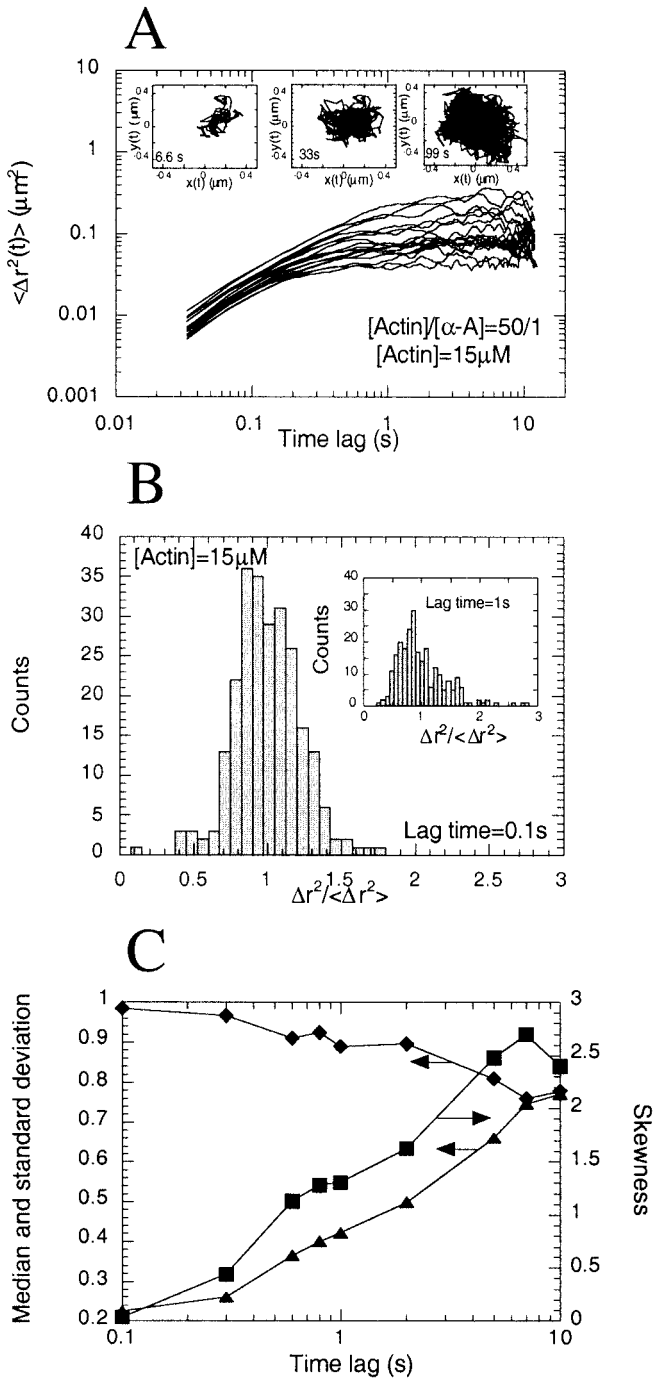

FIGURE 6 Principle of MPT analysis. (*A*) Randomly selected MSDs as a function of time lag. (*Insets*) Typical trajectory of a 0.97 μm-diameter, fluorescent, polystyrene bead imbedded in an F-actin/α-actinin network. The thermally excited motion of the bead was recorded for 6.6, 33, and 99 s, respectively. The bead's trajectory was captured by monitoring its intensity-weighted, centroid displacement via video fluorescence microscopy with a spatial resolution of ~5 nm (see Methods). (*B*) MSD distribution (n = 220 particles) measured at a time lag of 0.1 s, normalized by the corresponding ensemble-averaged mean. (*Inset*) Normalized MSD distribution measured at 1 s. (*C*) Median (♦), standard deviation (▲), and skewness (■) of the normalized MSD distribution as a function of time lag. Actin concentration was 15 μM; α-actinin concentration was 0.3 μM.

tration, however, the plateau at long time scales almost vanished (Fig. 7 *A*). For increasing actin (and α-actinin) concentrations, the MSD distributions became wide and skewed (compare Fig. 7, *C* and *D*). Further, for each tested specimen (Figs. 6 and 7), the asymmetry (measured by the skewness and the median) and the apparent width (measured by the standard deviation) of the MSD distribution steeply increased for increasing time lags (Figs. 6 *B* and 7, *C* and *D* to their respective *insets*).

For a fixed concentration of α-actinin and low actin concentration, the amplitude of the displacements of polystyrene beads dispersed in actin/α-actinin networks grew rapidly (Fig. 8 *A*, *inset*) and the associated MSD increased almost linearly over a wide range of time lags (Fig. 8 *A*). This is a hallmark of viscous behavior, for which the movement of a bead is purely diffusive and $\langle \Delta r^2(t) \rangle \sim t$ (Palmer et al., 1999; Berg, 1993). At high actin concentrations, however, the amplitude of the displacements (*insets*, Fig. 8 *C*), and therefore of the MSD, was vastly reduced and the MSD profiles reached a quasiplateau at long time scales (Fig. 8 *C*). The MSD distribution of this relatively concentrated solution was wider and more skewed than that of the more dilute specimen (Fig. 8, *B*, *D*, and *E*). For networks of fixed actin concentration and for increasing α-actinin concentration, the amplitude of the MSD slightly decreased (Fig. 9, *A* and *C*), and the MSD distributions became progressively wider and more skewed (Fig. 9, *B*, *D,* and *E*). Moreover, the MSD distributions became progressively wider and more asymmetric for increasing time lags, much more rapidly than for actin alone (Apgar et al., 2000; Fig. 9 *B*, *D*, and *E*). Therefore, increasing the concentration of F-actin or α-actinin in cross-linked actin filament networks typically enhanced the range of displacements and the asymmetry of the MSD distribution (see Fig. 10).

DISCUSSION

Previous in vivo mechanical studies suggest that the local organization and mechanical properties of the actin cytoskeleton can be regulated either by modulating the cytoplasmic content in F-actin or by changing the concentration in cross-linking proteins, or both. In focusing on the prototypical F-actin-cross-linking protein α-actinin, this paper reports a systematic study of the in vitro mechanical properties and microheterogeneity of F-actin/α-actinin networks of either fixed concentration of actin, fixed concentration of α-actinin, or fixed molar ratio of actin-to-α-actinin. A summary of the mechanical and microstructural properties of the F-actin/α-actinin networks solutions considered in this study is given in Fig. 11. We found that the three systems under investigation displayed very different concentration-dependent mechanical properties and degrees of microheterogeneity.

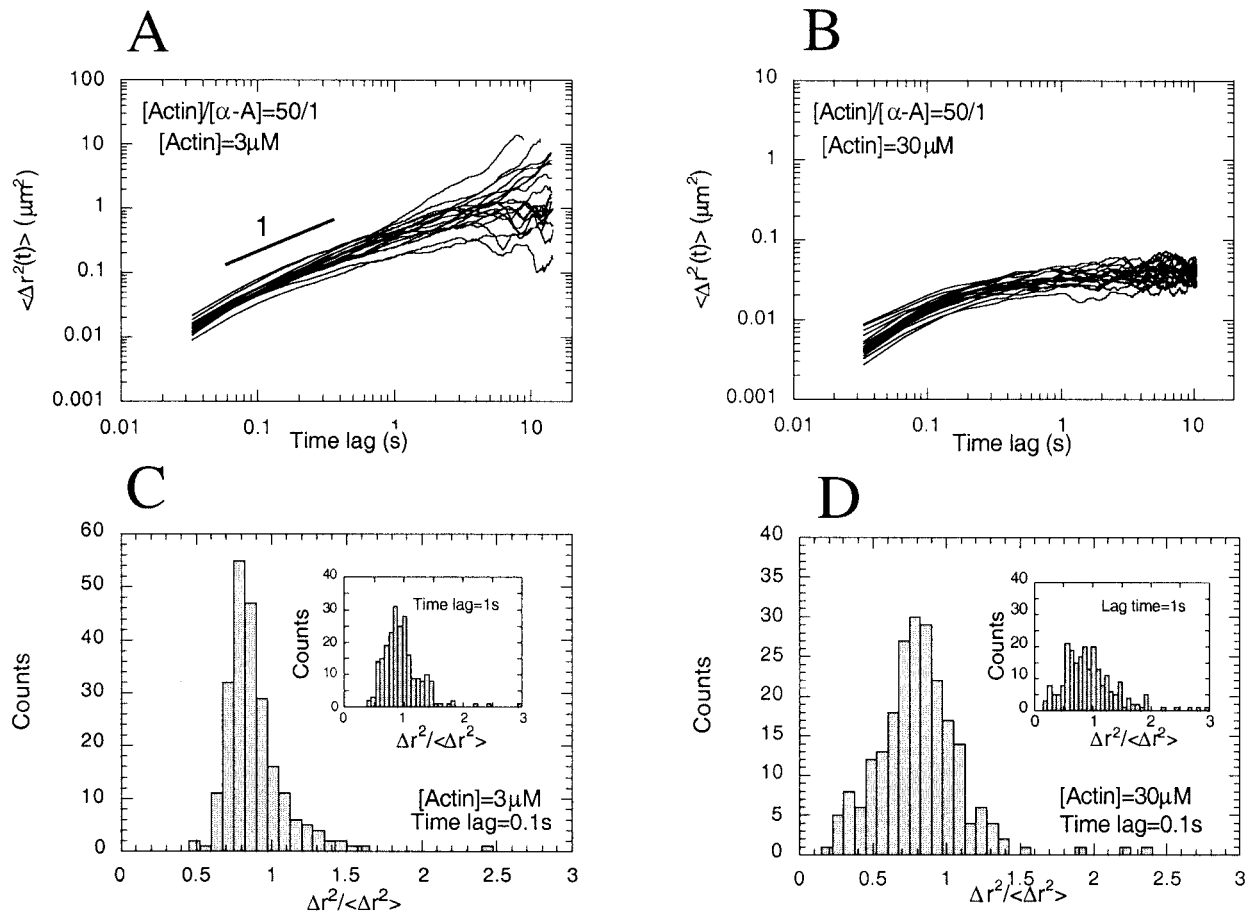

FIGURE 7 MPT analysis of F-actin/α-actinin networks of fixed actin-to-α-actinin molar ratio. (*A*) and (*B*) Randomly selected MSDs of 0.97 μm-diameter polystyrene beads for an actin concentration of (*A*) 3 μM and (*B*) 30 μM. (*C*) and (*D*) Corresponding MSD distributions (n = 230 particles) measured at a time lag of 0.1 s, normalized by the corresponding ensemble-averaged mean, for an actin concentration of (*C*) 3 μM and (*D*) 30 μM. The molar ratio of actin-to-α-actinin was 50:1 in all experiments.

Degree of heterogeneity in F-actin/α-actinin networks

Because local defects in an F-actin meshwork may constitute structurally weak points, they could greatly affect the global mechanical response of the network, which may soften earlier or enhance the elasticity less rapidly than predicted for increasing polymer concentration than for a network of uniform mesh size. In the absence of F-actin cross-linking proteins, actin filaments can ultimately diffuse (Kas et al., 1994), which renders the network uniform; one therefore expects that the local heterogeneities that appear during network gelation will vanish over time. Our results show that the addition of α-actinin to an actin filament suspension increases the standard deviation and asymmetry of the MSD distribution (Fig. 7). This is attributable to the fact that, for an increasing concentration of α-actinin, the homogenization of the meshwork becomes compromised as all α-actinin molecules bound to a filament have to collectively come off that filament to let it diffuse (Xu et al., 1998b, 2000). This collective lifetime of binding is predicted to increase exponentially with the number of cross-linkers per filaments (Leibler et al., 1991). Hence, despite the fact that networks are allowed to relax overnight (see Methods), defects created during F-actin/α-actinin network gelation, which creates a nonuniform mesh size, become very stable.

The difference between the widths of the MSD distributions of cross-linked and uncross-linked networks is accentuated at long time scales. This result is expected because beads embedded in a nonuniform network will reach increasingly different plateau values at long time scales. The displacements of a bead entropically trapped in a local "cage" created by overlapping filaments and bundles will remain limited, whereas the displacements of beads initially in a large polymer-free pocket will grow rapidly with time lag (Apgar et al., 2000).

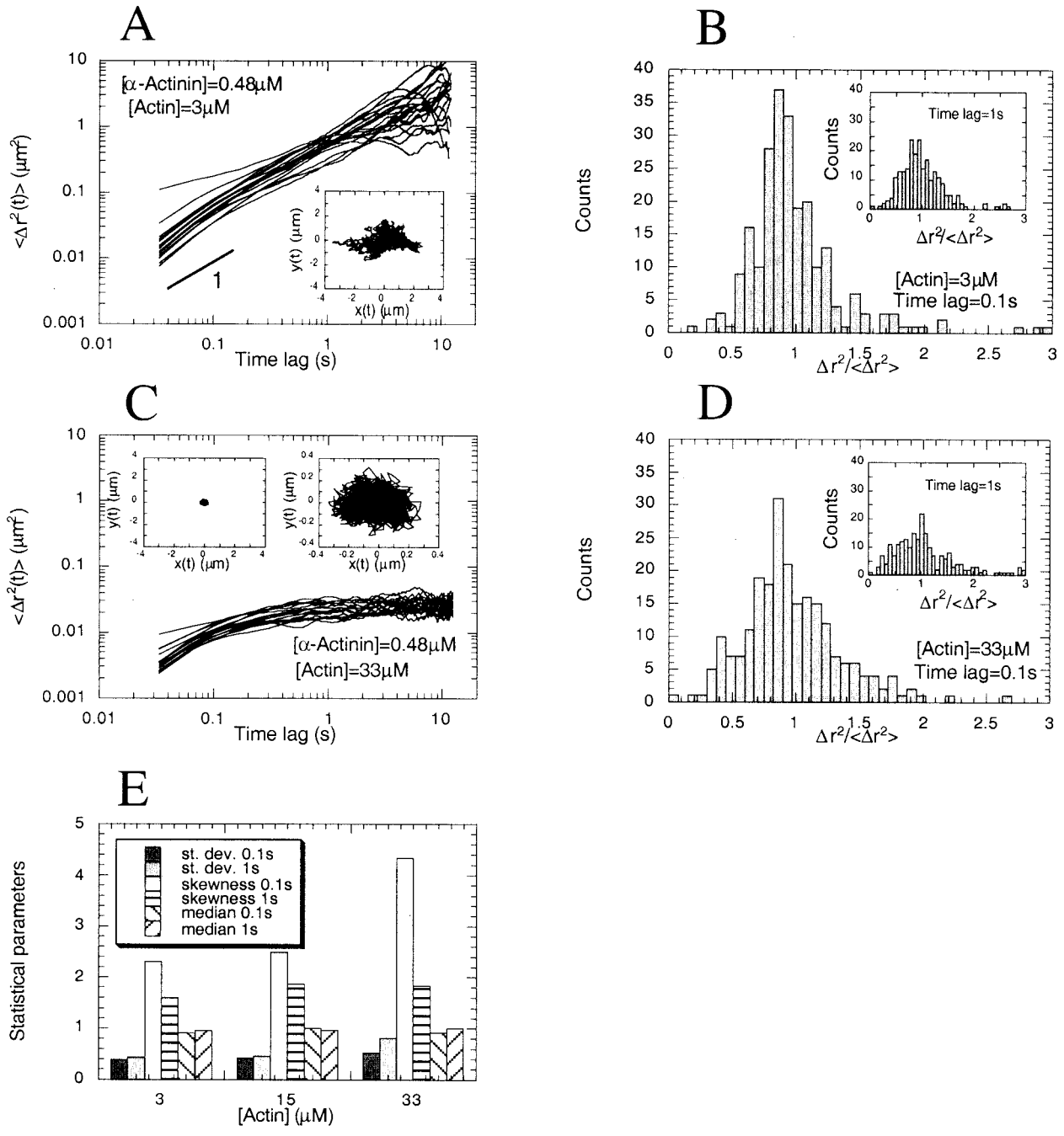

FIGURE 8 MPT analysis of F-actin/α-actinin networks of fixed α-actinin concentration. (*A*) Randomly selected MSDs, as a function of time lag, of 0.97 μm-diameter polystyrene beads dispersed in a F-actin/α-actinin solution of 3 μM actin concentration. (*Inset*) Typical trajectory of a bead recorded for 10 s. (*B*) Corresponding MSD distributions ($n = 230$ particles) measured at a time lag of 0.1 s and 1 s (*inset*), normalized by the ensemble-averaged mean. (*C*) and (*D*) MSDs and MSD distributions collected at time lags of 0.1 s and 1 s (*inset*) for an actin concentration of 33 μM. (*Insets*) Typical trajectory of a single bead, recorded for 99 s, displayed at two length scales. (*E*) Median, standard deviation, and skewness of the normalized MSD distributions ($n = 230$), measured at the time lags of 0.1 and 1 s, as a function of actin concentration. α-Actinin concentration was 0.48 μM in all experiments.

Enhanced cross-linking versus enhanced heterogeneity

A recent model (MacKintosh et al., 1995), which implicitly assumes perfect network homogeneity, predicts that the elastic modulus of a cross-linked network of semiflexible polymers increases with actin concentration as $G'(c) \sim c^{2.25}$. This model was originally designed to describe the elasticity of an uncross-linked F-actin network. However,

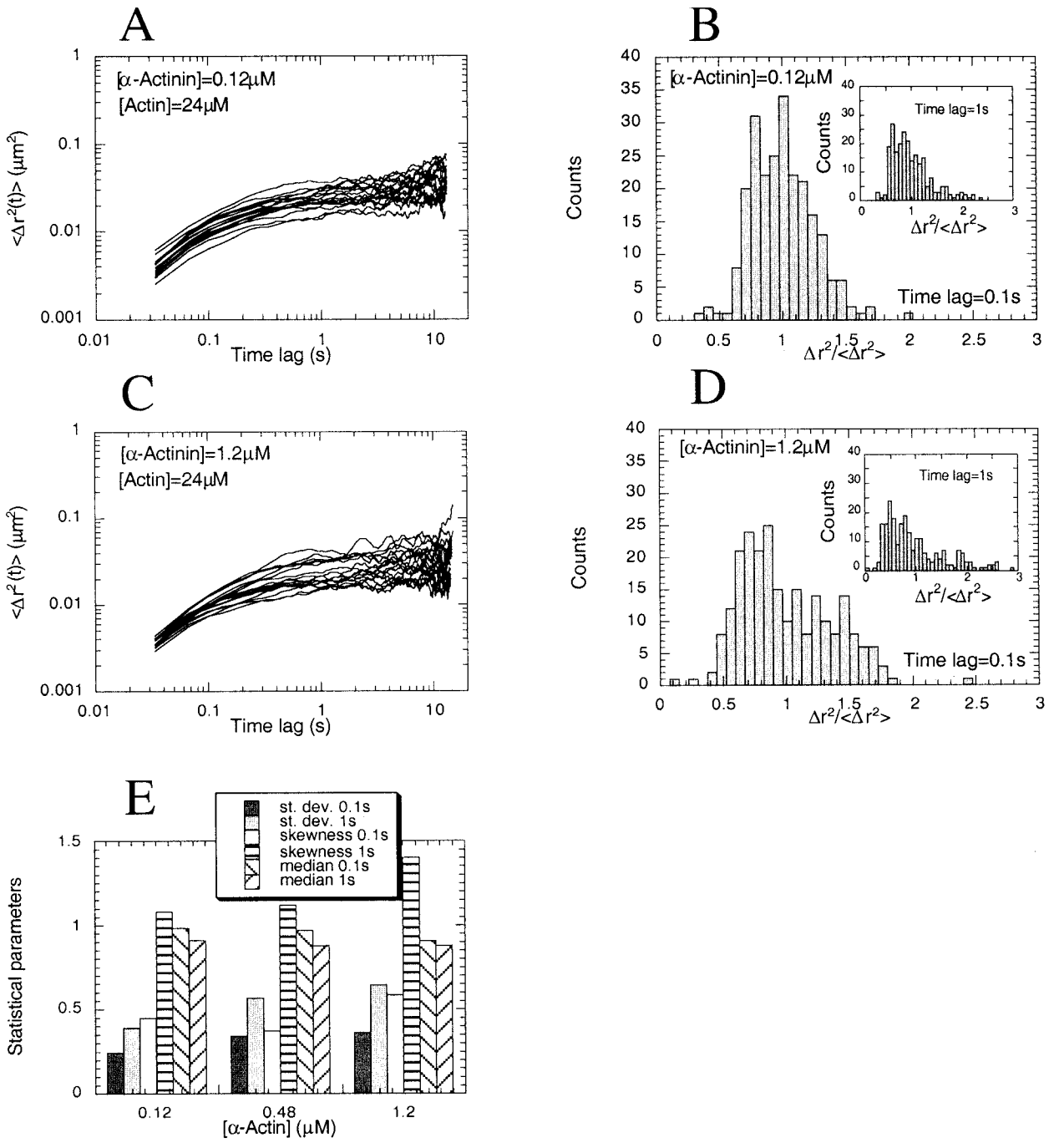

FIGURE 9 MPT analysis of F-actin/α-actinin networks of fixed actin concentration. (*A*) Randomly selected MSDs of 0.97 μm-diameter polystyrene beads dispersed in an F-actin solution of α-actinin concentration of 0.12 μM. (*B*) corresponding MSD distributions ($n = 240$) measured at a time lag of 0.1 s and 1 s (*inset*), normalized by the ensemble-averaged mean, for an α-actinin concentration of 0.12 μM. (*C*) and (*D*) MSDs and MSD distributions ($n = 240$), collected at time lags 0.1 s and 1 s (*inset*), for an α-actinin concentration of 1.2 μM. (*E*) Median, standard deviation, and skewness of the normalized MSD distributions ($n = 240$), measured at the time lags of 0.1 and 1 s, as a function of α-actinin concentration. Actin concentration was 24 μM in all experiments.

the fundamental mechanisms underlying the model involve bending fluctuations of the filaments and restricted longitudinal motion between entanglements, which are now believed to describe the entropic origin of elasticity in cross-linked F-actin solutions (Morse, 1998c; Palmer et al., 1998b). The concentration-dependence of the elastic modulus predicted by the model (MacKintosh et al., 1995) is much stronger than the measured concentration-depen-

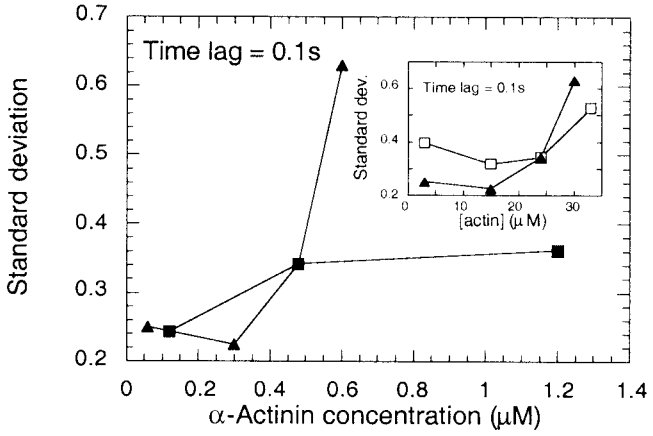

FIGURE 10 Concentration-dependent MPT microheterogeneity. Standard deviation of the MSD distribution measured at a time lag of 0.1 s as a function of α-actinin concentration. (*Inset*) Standard deviation of the MSD distribution as a function of actin concentration. Symbols correspond to F-actin/α-actinin solutions of fixed actin concentration (24 μM) (■), fixed molar ratio of actin-to-α-actinin (50:1) (▲), and fixed α-actinin concentration (0.48 μM) (□).

dence, $G'(c) \sim c^{1.71}$, obtained here with cross-linked networks of F-actin with a fixed number of α-actinin molecules per filament, the case closest to that considered in the model. The origin of this difference is suggested by our MPT data, which show that the simultaneous increase in the concentration of filaments and α-actinin enhances the standard deviation of the MSD distribution (Fig. 10). This suggests a progressive increase of the degree of heterogeneity (i.e., defects) in the gels, which, in turn, limits the rate of increase of G' with actin concentration compared with perfectly homogeneous gels.

We now discuss the dynamics, rheology, and microheterogeneity of the two other F-actin/α-actinin systems (i.e., fixed F-actin and fixed α-actinin concentrations). The elasticity of a cross-linked actin filament network stems from the inhibited movement of the filaments in solution. At very short time scales, actin filaments relax the stress mostly via bending fluctuations between entanglements (Morse, 1998a; Gittes and MacKintosh, 1998; Palmer et al., 1999, 1998b), which gives rise to the frequency dependence of the moduli at high frequencies (Fig. 5). At longer times scales, but shorter than the lifetime of binding of α-actinin to F-actin, longitudinal diffusion (so-called reptation) is prohibited, which produces a plateau modulus at intermediate frequencies (de Gennes, 1991). At a fixed temperature (Xu et al., 1998d), the collective lifetime of binding of α-actinin to F-actin depends mostly on its concentration and the binding lifetime is predicted to increase exponentially with the density of cross-linkers per filament (Leibler et al., 1991). Therefore, for a fixed concentration of F-actin, an increasing concentration of α-actinin will push the onset of the plateau modulus toward short time scales or, equivalently, toward high frequencies (Palmer et al., 1998b). The amplitude of the plateau modulus should increase, and, over a fixed range of frequencies (1–100 rad/s), the dynamic exponent a should decrease for increasing α-actinin con-

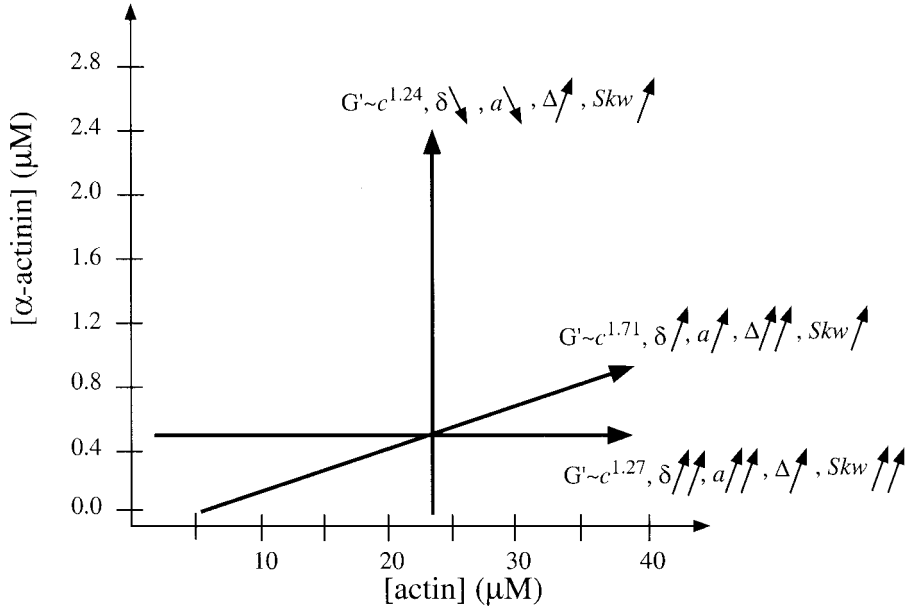

FIGURE 11 Summary of the concentration-dependent rheological and MPT microheterogeneity properties of the F-actin/α-actinin systems considered in the paper. *Long arrows* indicate the ranges of protein concentrations (actin, α-actinin, or both). The symbols G', δ, and a represent the elastic modulus, the phase angle (both measured at 1 rad/s), and the dynamic exponent determined by rheology; Δ and *Skw* represent the standard deviation and the skewness of the MSD distributions (measured at 1 s) determined by MPT. *One* and *two arrows*, respectively, indicate a mild and strong change in the rheological and statistical parameters with protein concentration.

centration, two predictions that are directly supported by our rheological measurements (Figs. 3 *B* and 5 *D*). This mechanism for reduced filament dynamics clearly dominates α-actinin-mediated F-actin bundling (which is detected by an increase in the phase-angle (Wachsstock et al., 1993)), which creates microscopic heterogeneities that enhance polymer dynamics (Figs. 1 and 10; Apgar et al., 2000).

For a fixed concentration of α-actinin, two competing mechanisms are at work. A relative decrease of the number of α-actinin molecules per filament will tend to make polymers progressively more mobile, i.e., the exponent a should increase with actin concentration. This mechanism is further enhanced by the decrease of the degree of heterogeneity of particle displacements (Fig. 8). Our results suggest that these effects overcome the decrease in the mesh size of the network induced by the increase in polymer concentration, which would reduce the propensity of the filaments to diffuse, which, in turn, would decrease the dynamic exponent a (Fig. 5, *E* and *F*). This last effect is small because the concentration dependence of the mesh size, $\xi(c) \sim c^{-0.25}$, is very weak for networks of semiflexible polymers (Isambert and Maggs, 1996).

Implications for the cell

Our results show that, together, the two structural proteins F-actin and α-actinin display an extremely wide variety of mechanical properties. These results suggest that the regulation of the expression of these two proteins, their affinity to one another, and their translocation to the actin-rich cortex, focal adhesions, and stress fibers, to which these two proteins colocalize (Kreis and Vale, 1999), provide the cell with an unsuspected range of regulatory pathways to modulate the cytoskeleton micromechanics, and, in turn, cell adhesion and cell migration (Gluck and Ben-Ze'ev, 1994). Given the long time necessary for gel stabilization (Fig. 2) and the in vivo localization of α-actinin, the results obtained in this paper mostly describe long-lived, α-actinin-rich actin structures, including focal adhesions and stress fibers, not the Arp2/3 complex-rich edge of the cell, which is highly homogeneous and dynamic (Svitkina and Borisy, 1999; Verkhovsky et al., 1995). Our rheological results further suggest that the cytoskeletal actin network will more rapidly enhance its stiffness by increasing the concentrations of actin and α-actinin simultaneously than by separately increasing the concentrations of actin and α-actinin, but at the cost of progressively creating more heterogeneous networks.

Our MPT measurements in vitro suggest that an increase in α-actinin will affect the microhomogeneity and associated micromechanical properties of the actin filament network in vivo. Recent in vivo measurements support our in vitro results. We applied laser-deflection particle tracking to monitor the Brownian motion of small, endogenous granules imbedded in the cytoskeleton of a COS7 cell and to measure in situ the local mechanical properties (Yamada et al., 2000). By reanalyzing these particle tracking measurements, we find that the granules imbedded in the perinuclear region of the cell exhibit a wide range of displacements, and, therefore, a large normalized standard deviation, namely 0.71 and 0.75 for time scales 0.1 and 1 s, respectively (Fig. 7 (Yamada et al., 2000)). We note that these standard deviations are similar to those measured for particles imbedded in F-actin networks in the presence of the cross-linking/bundling protein α-actinin (Figs. 6–9), but much smaller than measured in actin filament networks in the presence of the bona fide F-actin bundling protein fascin (Apgar et al., 2000). In contrast, particles imbedded in the lamellae showed a tight MSD distribution, with a normalized standard deviation of 0.58 and 0.65 for the time scales of 0.1 and 1 s, respectively. This difference in the widths of the MSD distributions correlates with the local degree of heterogeneity of the cytoskeletal actin filament network. Fluorescence and cryoelectron microscopies indeed show a highly heterogeneous network of stress fibers intertwined with unbundled F-actin in the perinuclear region of the cell and a relatively homogeneous actin network in the lamellae (Fig. 8 in (Yamada et al., 2000)).

By combining fluorimetry, cryoelectron microscopy, and in vivo MPT, we are currently testing whether the local concentrations in actin and α-actinin (and other actin cross-linking and bundling proteins) in a cell correlate with local changes in the width and asymmetry of the MSD distribution of microorganelles or exogenous microspheres. Our particle-tracking method could therefore be used not only to measure the local micromechanical properties of living cells (Bausch et al., 1999; Yamada et al., 2000), but also to quantify the degree of microheterogeneity of cytoplasm (Luby-Phelps et al., 1987; Jones and Luby-Phelps, 1996).

We thank Soichiro Yamada, Fred MacKintosh, and G. Borisy for insightful comments and acknowledge financial support from the National Science Foundation (grants CTS9812624, CTS0072278, and DB19729358).

REFERENCES

Amblard, F., A. C. Maggs, B. Yurke, A. N. Pargellis, and S. Leibler. 1996. Subdiffusion and anomalous local viscoelasticity in actin networks. *Phys. Rev. Lett.* 77: 4470–4473.

Apgar, J., Y. Tseng, E. Federov, M. B. Herwig, S. C. Almo, and D. Wirtz. 2000. Multiple-particle tracking measurements of the heterogeneities of solutions of actin filaments and actin bundles. *Biophys. J.* 79: 1095–1106.

Bausch, A. R., W. Môller, and E. Sackmann. 1999. Measurement of local viscoelasticity and forces in living cells by magnetic tweezers. *Biophys. J.* 76:573–579.

Berg, H. C. 1993. Random Walks in Biology. Princeton University Press, Princeton, NJ.

Borisy, G. G., and T. M. Svitkina. 2000. Actin machinery: pushing the envelope. *Cur. Opin. Cell Biol.* 12:104–112.

Cortese, J. D., and C. Frieden. 1988. Microheterogeneity of actin gels formed under controlled linear shear. *J. Cell Biol.* 107:1477–1487.

Cortese, J. D., and C. Frieden. 1990. Effect of filamin and controlled linear shear on the microheterogeneity of F-actin/gelsolin gels. *Cell Motil. Cytoskeleton.* 17:236–249.

Coulombe, P. A., O. Bousquet, L. Ma, S. Yamada, and D. Wirtz. 2000. The 'ins' and 'outs' of intermediate filament organization. *Trends Cell. Biol.* 10:420–428.

de Gennes, P.-G. 1991. Scaling Concepts in Polymer Physics. Cornell University Press, Ithaca.

Ferry, J. D. 1980. Viscoelastic Properties of Polymers. John Wiley and Sons, New York.

Gittes, F., and F. C. MacKintosh. 1998. Dynamic shear modulus of a semiflexible polymer network. *Phys. Rev. E.* 58: R1241–1244.

Gittes, F., B. Schnurr, P. D. Olmsted, F. C. MacKintosh, and C. F. Schmidt. 1997. Microscopic viscoelasticity: shear moduli of soft materials determined from thermal fluctuations. *Phys. Rev. Lett.* 79:3286–3289.

Gluck, U., and A. Ben-Ze'ev. 1994. Modulation of α-actinin levels affects cell motility and confers tumorigenicity on 3T3 cells. *J. Cell Sci.* 107:1773–1782.

Gluck, U., J. L. Rodriguez Fernandez, R. Pankov, and A. Ben-Ze'ev. 1992. Regulation of adherens junction protein expression in growth-activated 3T3 cells and in regenerating liver. *Exp. Cell Res.* 202:477–486.

Grazi, E., P. Cuneo, E. Magri, C. Schwienbacher, and G. Trombetta. 1993. Diffusion hindrance and geometry of filament crossings account for the complex interactions of F-actin with α-actinin from chicken gizzard. *Biochemistry.* 32:8896–8901.

Isambert, H., and A. C. Maggs. 1996. Dynamics and rheology of actin solutions. *Macromolecules.* 29:1036–1040.

Janmey, P. A., S. Hvidt, J. Lamb, and T. P. Stossel. 1990. Resemblance of actin-binding protein/actin gels to covalently crosslinked networks. *Nature.* 345:89–92.

Jones, J. D., and K. Luby-Phelps. 1996. Tracer diffusion through F-actin: effect of filament length and cross-linking. *Biophys. J.* 71:2742–2750.

Kas, J., H. Strey, and E. Sackmann. 1994. Direct imaging of reptation for semiflexible actin filaments. *Nature.* 368:226–229.

Kirkeeide, E. K., I. F. Pryme, and A. Vedeler. 1993. Microfilaments and protein synthesis; effects of insulin. *Int. J. Biochem.* 25:853–864.

Kreis, T., and R. Vale. 1999. Guidebook to the Cytoskeletal and Motor Proteins. Oxford University Press, Oxford.

Leduc, P., C. Haber, G. Bao, and D. Wirtz. 1999. Dynamics of individual flexible polymers in a shear flow. *Nature.* 399:564–566.

Leibler, L., M. Rubinstein, and R. H. Colby. 1991. Dynamics of reversible networks. *Macromolecules.* 24:4701–4707.

Luby-Phelps, K., P. E. Castle, D. L. Taylor, and F. Lanni. 1987. Hindered diffusion of inert tracer particles in the cytoplasm of mouse 3T3 cells. *Proc. Natl. Acad. Sci. U.S.A.* 84: 4910–4913.

Ma, L., J. Xu, P. A. Coulombe, and D. Wirtz. 1999. Epidermal keratin suspensions have unique micromechanical properties. *J. Biol. Chem.* 274:19145–19151.

Ma, L., S. Yamada, D. Wirtz, and P. A. Coulombe. 2001. A 'hot-spot' mutation alters the mechanical properties of keratin filament networks. *Nat. Cell Biol.* 3:503–506.

MacKintosh, F. C., J. Kas, and P. A. Janmey. 1995. Elasticity of semiflexible biopolymer networks. *Phys. Rev. Lett.* 75:4425–4428.

Maksym, G. N., B. Fabry, J. P. Butler, D. Navajas, D. J. Tschumperlin, J. D. Laporte, and J. J. Fredberg. 2000. Mechanical properties of cultured human airway smooth muscle cells from 0.05 to 0.4 Hz. *J. Appl. Physiol.* 89:1619–1632.

Mason, T. G., A. Dhople, and D. Wirtz. 1997a. Concentrated DNA rheology and microrheology. *In* Statistical Mechanics in Physics and Biology. D. Wirtz and T. C. Halsey, editors. 153–158.

Mason, T. G., K. Ganesan, J. V. van Zanten, D. Wirtz, and S. C. Kuo. 1997b. Particle-tracking microrheology of complex fluids. *Phys. Rev. Lett.* 79:3282–3285.

Merkel, R., R. Simson, D. A. Simson, M. Hohenadl, A. Boulbitch, E. Wallraff, and E. Sackmann. 2000. A micromechanic study of cell polarity and plasma membrane cell body coupling in *Dictyostelium*. *Biophys. J.* 79:707–719.

Morse, D. C. 1998a. Viscoelasticity of concentrated isotropic solutions of semiflexible polymers. 1. Model and stress tensor. *Macromolecules.* 31:7030–7043.

Morse, D. C. 1998b. Viscoelasticity of concentrated isotropic solutions of semiflexible polymers. 2. Linear response. *Macromolecules.* 31: 7044–7067.

Morse, D. C. 1998c. Viscoelasticity of tightly entangled solutions of semiflexible polymers. *Phys. Rev. E.* 58:R1237–R1240.

Myers, J. C., D. Li, N. A. Rubinstein, and C. C. Clark. 1999. Up-regulation of type XIX collagen in rhabdomyosarcoma cells accompanies myogenic differentiation. *Exp. Cell Res.* 253:587–598.

Palmer, A., B. Cha, and D. Wirtz. 1998a. Structure and dynamics of actin filament solutions in the presence of latrunculin A. *J. Polym. Sc. Physics Ed.* 36:3007–3015.

Palmer, A., J. Xu, S. C. Kuo, and D. Wirtz. 1999. Diffusing wave spectroscopy microrheology of actin filament networks. *Biophys. J.* 76:1063–1071.

Palmer, A., J. Xu., and D. Wirtz. 1998b. High-frequency rheology of crosslinked actin networks measured by diffusing wave spectroscopy. *Rheologica Acta.* 37:97–108.

Pollard, T. D., S. Almo, S. Quirk, V. Vinson, and E. E. Lattman. 1994. Structure of actin binding proteins: insights about function at atomic resolution. *Annu. Rev. Cell Biol.* 10:207–249.

Pollard, T. D., L. Blanchoin, and R. D. Mullins. 2000. Molecular mechanisms controlling actin filament dynamics in nonmuscle cells. *Annu. Rev. Biophys. Biomol. Struct.* 29:545–576.

Rodriguez Fernandez, J. L., and A. Ben-Ze'ev. 1989. Regulation of fibronectin, integrin and cytoskeleton expression in differentiating adipocytes: inhibition by extracellular matrix and polylysine. *Differentiation.* 42:65–74.

Rufener, K., A. Palmer, J. Xu, and D. Wirtz. 1999. High-frequency dynamics and microrheology of macromolecular solutions measured by diffusing wave spectroscopy: the case of actin filament networks. *J. Non-Newtonian Fluid Mech.* 82:303–314.

Sato, M., W. H. Schwarz, and T. D. Pollard. 1987. Dependence of the mechanical properties of actin/α-actinin gels on deformation rate. *Nature.* 325:828–830.

Schnurr, B., F. Gittes, F. C. MacKintosh, and C. F. Schmidt. 1997. Determining microscopic viscoelasticity in flexible and semiflexible polymer networks from thermal fluctuations. *Macromolecules.* 30: 7781–7792.

Small, J. V., K. Rottner, and I. Kaverina. 1999. Functional design in the actin cytoskeleton. *Curr. Opin. Cell Biol.* 11:54–60.

Spudich, J. A., and S. Watt. 1971. The regulation of rabbit skeletal muscle contraction. *J. Biol. Chem.* 246:4866–4871.

Svitkina, T. M., and G. G. Borisy. 1999. Arp2/3 complex and actin depolymerizing factor/cofilin in dendritic organization and treadmilling of actin filament array in lamellipodia. *J. Cell Biol.* 145:1009–1026.

Tempel, M., G. Isenberg, and E. Sackmann. 1996. Temperature-induced sol-gel transition and microgel formation in α-actinin cross-linked actin networks: a rheological study. *Phys. Rev. E.* 54:1802–1808.

Verkhovsky, A. B., T. M. Svitkina, and G. G. Borisy. 1995. Myosin II filament assemblies in the active lamella of fibroblasts: their morphogenesis and role in the formation of actin filament bundles. *J. Cell Biol.* 131:989–1002.

Wachsstock, D., W. H. Schwarz, and T. D. Pollard. 1993. Affinity of α-actinin for actin determines the structure and mechanical properties of actin filament gels. *Biophys. J.* 65:205–214.

Wachsstock, D., W. H. Schwarz, and T. D. Pollard. 1994. Cross-linker dynamics determine the mechanical properties of actin gels. *Biophys. J.* 66:801–809.

Xu, J., A. Palmer, and D. Wirtz. 1998a. Rheology and microrheology of semiflexible polymer solutions: actin filament networks. *Macromolecules.* 31:6486–6492.

Xu, J., W. H. Schwarz, J. Kas, P. J. Janmey, and T. D. Pollard. 1998b. Mechanical properties of actin filament networks depend on preparation, polymerization conditions, and storage of actin monomers. *Biophys. J.* 74:2731–2740.

Xu, J., Y. Tseng, and D. Wirtz. 2000. Strain hardening of actin filament networks. Regulation by the dynamic cross-linking protein α-actinin. *J. Biol. Chem.* 275:35886–35892.

Xu, J., V. Viasnoff, and D. Wirtz. 1998c. Compliance of actin filament networks measured by particle-tracking microrheology and diffusing wave spectroscopy. *Rheologica Acta.* 37:387–398.

Xu, J., D. Wirtz, and T. D. Pollard. 1998d. Dynamic cross-linking by α-actinin determines the mechanical properties of actin filament networks. *J. Biol. Chem.* 273:9570–9576.

Yamada, S., D. Wirtz, and S. C. Kuo. 2000. Mechanics of living cells measured by laser tracking microrheology. *Biophys. J.* 78: 1736–1747.